

Generation of extreme state of water by spherical wire array underwater electrical explosion

O. Antonov, L. Gilburd, S. Efimov, G. Bazalitski, V. Tz. Gurovich, and Ya. E. Krasik
 Physics Department, Technion, Haifa 3200, Israel

(Received 23 August 2012; accepted 25 September 2012; published online 8 October 2012)

The results of the first experiments on the underwater electrical explosion of a spherical wire array generating a converging strong shock wave are reported. Using a moderate pulse power generator with a stored energy of ≤ 6 kJ and discharge current of ≤ 500 kA with a rise-time of ~ 300 ns, explosions of Cu and Al wire arrays of different diameters and with a different number and diameter of wires were tested. Electrical, optical, and destruction diagnostics were used to determine the energy deposited into the array, the time-of-flight of the shock wave to the origin of the implosion, and the parameters of water at that location. The experimental and numerical simulation results indicate that the convergence of the shock wave leads to the formation of an extreme state of water in the vicinity of the implosion origin that is characterized by pressure, temperature, and compression factors of $(2 \pm 0.2) \times 10^{12}$ Pa, 8 ± 0.5 eV, and 7 ± 0.5 , respectively. © 2012 American Institute of Physics. [<http://dx.doi.org/10.1063/1.4757984>]

The generation of extreme states of matter is attracting continuous interest among researchers in the fields of high energy density physics¹ and warm dense matter related to the physics of giant planets,² the equation of states (EOS), the conductivity of matter in extreme conditions,³ and the hydrodynamics of fuel pellets for inertial confinement fusion.⁴ Different approaches, namely, chemical explosions, pulsed powerful lasers, light multistage gas guns, z-pinches, and magneto-explosive generators allow one to achieve a pressure $\geq 10^{11}$ Pa. For instance, a two-stage light-gas gun, powerful laser beams, a pulsed power Z-generator at Sandia, and laser- or magnetically driven shock waves were used to study electrical conductivity^{5,6} and phase transitions⁷ of either water or deuterium⁸ at extreme conditions, the physics of radiative shock waves in gas,⁹ and the convergence of strong shock waves (SSW) in water.¹⁰ These experiments revealed that at extreme conditions, water transforms to solid ice and becomes a rather good conductor. In addition, new data concerning EOS for water and deuterium liquid were obtained. This experimental research was carried out using large facilities with stored energy of ≥ 100 kJ. Recently, it was shown that using a moderate pulse power generator with stored energy of only a few kJ, the underwater electrical explosion of a cylindrical wire array results in the generation of converging SSW.¹¹ Hydrodynamic (HD) simulations coupled with the experimental data and EOS for water showed that this SSW generates extremely large pressure, $\leq 6 \times 10^{11}$ Pa, in the vicinity of the implosion axis.

In this letter, we present the results of the first experiments on underwater electrical explosion of a spherical wire array. The underwater electrical explosion of wires causes individual SSWs to be generated whose overlapping leads to the formation of a converging SSW.¹¹ Such an SSW can produce a larger pressure in the vicinity of the origin of the implosion than does a cylindrical SSW. Self-similarity analysis¹² reveals that the pressure, p_s , at the front of the spherical SSW at a location with radius r_c is $p_s \propto (r_0^{0.34} \cdot r_c^{0.66})p_{cyl}$,

where p_{cyl} is the pressure at the front of the cylindrical SSW that reaches r_c , and r_0 is the “initial” self-similar SSW radius. Thus, when an identical energy is deposited into the water flow and for the same value of r_0 , for instance $r_0 = 10^4 \mu\text{m}$, one obtains an enhancement of the pressure by ~ 100 in the case of a spherical SSW converged to $r_c = 10 \mu\text{m}$.

The experiments were carried out using a pulsed generator¹¹ with stored energy of ~ 6 kJ at an 80 kV charging voltage, delivering a current of ~ 500 kA with a rise-time of ~ 300 ns to the spherical wire array. In the experiments, wire arrays 20 mm, 30 mm, and 40 mm in diameter were tested, with the number of either Cu or Al wires being in the range 20–40 and wire diameters in the range 114–160 μm . To prepare the wire array, a ball made of organic material with a polar hole was used. Two electrodes, each 10 mm in diameter, having central holes, were placed at the poles of the ball and fixed by a central rod. The wires were stretched between the electrodes uniformly. The array was then fixed by dielectric posts and the rod was removed. This array was placed in a cavity filled with acetone that dissolved the ball, leaving a spherical form of wires. Next, the array was placed between the generator’s high-voltage (HV) and grounded electrodes, which were immersed in de-ionized water (total volume of ~ 0.4 l) (Fig. 1).

The current, $I(t)$, and resistive voltage, $\varphi_r(t)$, measured by a calibrated D-dot and two B-dot probes, respectively,¹¹ were used to calculate the energy deposition into the exploding wires (see Fig. 2). The explosion is characterized by an aperiodic discharge with $I \approx 510$ kA and wire array resistance of $\sim 0.15 \Omega$ at the time of maximum value of φ_r . The maximal delivered power is ~ 30 GW, and $\sim 87\%$ of the stored energy is absorbed by the exploding wire array during ~ 700 ns of the discharge. Almost the same electrical parameters were obtained for explosions of 30 mm and 40 mm in diameter Al and Cu wire arrays, respectively. In the case of the 20 mm-diameter Cu wire arrays, in spite of a smaller charging voltage of 70 kV, the current was ~ 475 kA due to

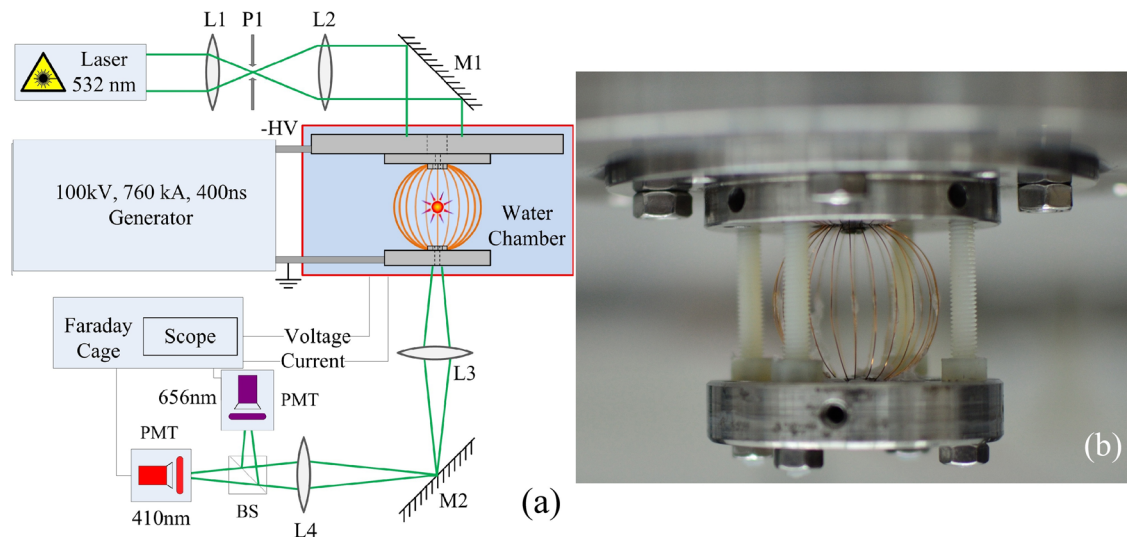


FIG. 1. (a). Experimental setup. (b) External view of 40 Cu wires array of 30 mm in diameter; each wire is of 114 μm in diameter.

the decrease in the load inductance. However, in this case, ringing of the current was obtained, which results in a $\sim 30\%$ decrease in the deposited energy.

The time-of-flight (TOF) of the converging SSW was determined by the beginning of water light emission in the vicinity of the sphere origin. This light emission was sampled along the viewing chord through the 1 mm in diameter and 15 mm in length collimator in the grounded electrode using two R7400U-04 photo-multiplier tubes (PMT), with an interference (± 5 nm) filter (either 410 nm or 656 nm), beam splitter, and lenses. For the 30 mm-diameter array, this setup allows one to obtain the light emission from a water volume having a diameter ~ 1.2 mm, whose origin is in the center of the sphere. PMT data were also used to estimate water temperature assuming black body (BB) radiation. The sensitivity of the PMTs was determined using an Oriol QTH 200 lamp. The TOF of the converging SSW was also obtained using 1 mm-diameter optical fiber covered by a non-transparent shrink tube. The fiber was placed either through the holes in the electrodes or through the space between the wires along the equatorial diameter of the sphere. The fiber outputs were attached to the interference filters. When the SSW approached the center of implosion, a strong light emission was obtained by both PMTs. A radial displacement of the fiber on ~ 0.5 mm of the axis led to either a drastic decrease in or even the disappearance of the light intensity. In addition, graphite rods with diameters in the range 0.5–2 mm and Al (0.5 mm in diameter) and Cu

(0.6 mm and 0.13 mm in diameter) wires inside shrink tubes were placed along equatorial diameter in order to obtain the pattern in which the maximal energy density deposition is realized.

The waveforms of the water and fiber light emission for the explosions of the 30 mm-diameter Cu wire array are shown in Fig. 3. Similar results were obtained in explosions of 20 mm- and 40 mm-diameter Cu wire arrays. The time delay of the appearance of the light emission of the water or fiber with respect to the beginning of the current was correlated only with the diameter of the array. The reproducibility (2–5 explosions for each array diameter) of the time delay for Cu wire array diameters of 20 mm, 30 mm, and 40 mm was $3 \pm 0.1 \mu\text{s}$, $6 \pm 0.2 \mu\text{s}$, and $8 \pm 0.2 \mu\text{s}$, respectively. In the 30 mm-diameter Al wire array explosions, the time delay was ~ 200 ns shorter than in explosions of a Cu wire array with the same diameter. These time delays for different array diameters were almost the same (time jitter ± 50 ns) whether the fiber was placed through the polar electrodes or along the equatorial diameter. The only difference that occurred was that when the fiber was placed through the polar electrodes, it was destroyed completely, whereas only the central part (≤ 1.5 mm in length) of the equatorially placed fiber was completely destroyed (see Fig. 4). The complete destruction of the polar-placed fiber is explained by its partial evaporation leading to an electrical discharge between the HV and grounded electrodes induced by the current (~ 10 kA) continuing to flow after the main discharge. A similar

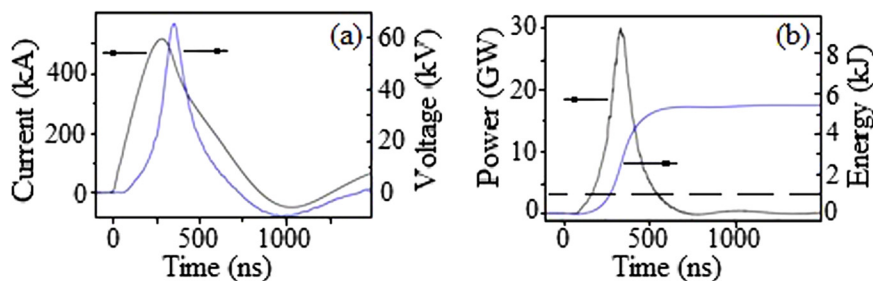


FIG. 2. Waveforms of (a) the current, resistive voltage, and (b) power and energy. 30 mm in diameter spherical Cu wire array; 40 wires each of 114 μm in diameter. Dotted line in (b) is the energy required for complete evaporation of Cu wires.

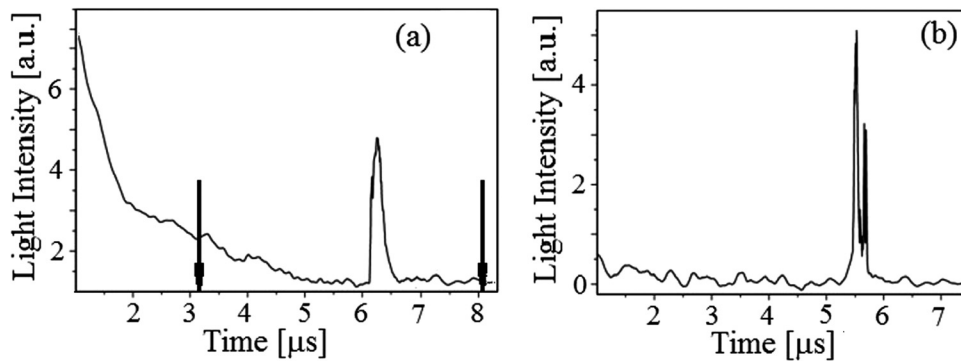


FIG. 3. Typical waveform of the (a) water and (b) fiber light emission. Explosion of Cu wire array. Arrows corresponds to the appearance of water light emission in the case of 20-mm- and 40-mm-diameter Cu wire array explosion.

destruction of the central parts was obtained in experiments tested with graphite rods, and Al and Cu (0.13 mm in diameter) wires; only the 0.6 mm-diameter Cu wire was not damaged (except for a damaged shrink tube in the central part).

The duration of the water and fiber light emission was 550 ± 250 ns and 300 ± 50 ns, respectively, which is ~ 10 times larger than in experiments with cylindrical wire array explosions.¹¹ These data indicate a larger energy deposition into the water at the origin of the implosion. In some explosions, two peaks in radiation were obtained [see Fig. 3(b)], which can be related to the non-uniform SSW implosion.

The main obstacle in this experimental research is the complexity of measuring the water and SSW parameters. Nevertheless, the scaling of the time delay of the appearance of the water or fiber light emission versus the wire array diameter (see Fig. 3(a)) indicates that the explosion of the wire array leads to the generation of converging SSW. The equality of the time delays in the light's appearance from the polar and equatorially placed fibers indicates spherical uniformity of the SSW along the main part of its convergence. Further, the obtained strong light emission from the water and fiber and the central damage of the equatorially placed fiber, graphite rods, and Al and Cu wires indicate that a high temperature and large pressure are generated in the vicinity of the implosion.

Thus, assuming spherical symmetry of the converging SSW, 1D HD simulations^{11,12} coupled to the SESAME EOS



FIG. 4. Equatorially placed fiber after the experiment with explosion of 30 mm in diameter Cu wire array.

for water, Cu, and Al were performed. The simulated volume was divided into the inner water layer inside the array, the exploding metallic layer, and the water layer outside the array. The SSW velocity was governed by the expansion of a metallic layer having the same mass (M_w) as the Cu wires. The deposition of the energy into the layer mass element dm was calculated as $d\omega/dt = \alpha\phi_r IM_w^{-1} dm$, where $\alpha < 0.5$ is the only fitting coefficient, which was used to obtain the best fit between the simulated and the experimental SSW TOF data. Different time and space steps and values of artificial viscosity were checked to obtain the width of the SSW front of $\sim 3 \mu\text{m}$ in the vicinity of the implosion origin, i.e., at the instant when the SSW reaches $r=0$, the maximum pressure at the SSW was at $r=3 \mu\text{m}$. The simulation results showed that the efficiency of the transfer of the energy deposited into the metallic layer to the energy of the converging water flow is $\leq 12\%$, which agrees with the experimental results presented in Ref. 13. In addition, it was shown that experimental errors in the TOF of the SSW of ± 150 ns and deposited energy of $\pm 5\%$ result in variations of $\pm 25\%$, $\pm 13\%$, and $\pm 8\%$ in the simulated water pressure, temperature, and compression ratio, respectively, in the vicinity of the origin. The examples of the results of these simulations (see Table I) showed that one can expect to obtain an extreme state of water in the vicinity of the origin of the implosion, especially immediately after the SSW is reflected from the origin of the implosion. In addition, simulation showed that the maximal pressure is realized in explosions of 20 mm-diameter Cu wire arrays, in spite of the smaller deposited energy than in explosions of 30 mm-diameter Cu wire arrays. In addition, a larger pressure is realized for the Al than for the Cu wire array explosion (for the same wire arrays diameter). This is explained by the additional energy deposited into the water flow due to Al wire combustion.¹⁴ The simulations also showed that in the case of explosion of the 20 mm-diameter Cu wire array, the state of water $P = 10^{12}$ Pa, $T = 5$ eV, and $\delta = 5$ could be realized in the volume with $r = 13 \mu\text{m}$ with a time duration of 17 ns.

However, these simulation results were obtained assuming SSW spherical uniformity, which could lead to the water parameters in the case of the SSW non-uniformity being significantly overestimated, especially at the final stage of implosion. Nevertheless, let us note that the simulations showed that a converging SSW, generated by the explosion of the cylindrical wire array with $r = 15$ mm and with the same energy deposition as in the spherical case, gives a SSW

TABLE I. Simulation results. Here, P_1 , T_1 , M , and δ_1 are the pressure, temperature, Mach number, and compression ratio at the front of the SSW ($r = 3 \mu\text{m}$) that reaches the origin of implosion, respectively; P_2 , T_2 , and δ_2 are the maximum pressure, temperature, and compression ratio that result from the SSW's reflection ($r = 3 \mu\text{m}$).

Array parameters	P_1 (10^{12} Pa)	P_2 (10^{12} Pa)	δ_1	δ_2	T_1 (eV)	T_2 (eV)	M
40 Cu wires, $\varnothing_w 114 \mu\text{m}$, $\varnothing_{ar} 20 \text{ mm}$	6.1	14.8	5.8	9.9	26.7	29	57
40 Cu wires, $\varnothing_w 114 \mu\text{m}$, $\varnothing_{ar} 30 \text{ mm}$	4.0	8.1	5.58	9.1	19	19	47
36 Al wires, $\varnothing_w 152 \mu\text{m}$, $\varnothing_{ar} 30 \text{ mm}$	6.2	16.7	5.8	10	27	32	58

TOF almost two times larger than experimental TOF data. This indicates that in the case of the spherical wire array explosion, the SSW keeps its uniformity along the main part of its convergence.

In fact, in spite of the prolonged research of converging either cylindrical or spherical SSW stability, there is no complete answer about the range of applicability and, respectively, the correctness of solutions for the limit of cumulations of cylindrical and spherical SSWs.^{17,18} For instance, in a review by Sokolov¹⁹ on this subject where different models of azimuthal instabilities are considered including models showing that in the case of the water, the converging shock wave is stable even in linear approximation and small perturbation can no limit cumulations. Therefore, for each experiment, this limit should be determined independently; we estimated water parameters in the vicinity of the origin based on the light emission from the water and the damaged central parts of fiber and Al and Cu wires placed along equatorial diameter.

First, let us estimate the temperature of water using data obtained by the PMTs with interference filters and assuming BB radiation gives a value ≤ 0.45 eV, which is significantly smaller than that of the simulation results. This apparent contradiction can be explained by the opaque effect of the surrounding "cold" plasma shell, similar to that analyzed in the research of light emission radiated by the exploding wire^{15,16} or by the water compressed by cylindrically converging SSW.¹¹ Nevertheless, assuming that a temperature of 0.45 eV is reached at the front of the SSW prior to the implosion and using the SESAME database, one obtains a pressure $\sim 10^{11}$ Pa. Even assuming two plane SSWs, immediately after the reflections from the origin, the pressure should increase to $\sim 6 \times 10^{11}$ Pa.

Now let us analyze the duration of the water light emission, which was 550 ± 250 ns. Using the data of the explosion of the 30 mm-diameter Cu wire array, namely, the PMT's waveform $\varphi_{PMT}(t)$, amplification $k = 10^6$, quantum efficiency of $\beta = 0.12$, and geometrical factor of light collection $\eta = 1.21 \times 10^4$, one can estimate the total flux of photons Y_γ emitted from the water during $t \approx 550 \pm 250$ ns as $Y_\gamma = (\eta \int_0^t \varphi_{PMT} dt) (R \beta k e)^{-1} \simeq (6 \pm 3) \times 10^8$, where $R = 50 \Omega$ is the PMT's load and e is the electron charge. Here the error bar in the total flux of photons is resulted from the error in duration and amplitude ($\pm 15\%$) of the waveform of the light emission obtained by the PMT. Thus, assuming BB radiation, the total flux of photons $Y_{\gamma BB} \approx 2\omega^2 \Delta\omega c^{-2} (e^{\hbar\omega/k_B T} - 1)^{-1} \int_0^t r^2(t) dt$ radiated in the spectral range 410 ± 5 nm ($\omega = 4.6 \times 10^{15} \text{ s}^{-1}$, $\Delta\omega = 5 \times 10^{13} \text{ s}^{-1}$) from the surface of the water sphere with variable radius $r(t)$ and

$T \approx 5000$ K should be equal to the value $Y_\gamma \simeq (6 \pm 3) \times 10^8$. Applying artificially decreased values of energy deposited into the wires, we used 1D HD simulations of spherically symmetrical SSW in order to obtain the parameters of water flow that would form a water sphere with a surface having $T = 5000$ K with a duration in the range 300–800 ns. Here, the decreased values of the deposited energy gives a much less intense SSW used to "model" the possible non-symmetry of the converging SSW, which should result in lower water parameter values at the origin of the convergence. The results of these simulations showed that only in the case when the deposited energy was decreased to $10\% \pm 2\%$ of the measured deposited energy does one obtain the required flux of photons, i.e., $Y_{\gamma BB} \approx 3 \times 10^8$ for duration of 300 ns and $Y_{\gamma BB} \approx 9 \times 10^8$ for duration of 800 ns. In this case, the results of simulations showed that the parameters of water for duration of light emission of 550 ± 250 ns are $P_1 \simeq (1 \pm 0.1) \times 10^{12}$ Pa, $T_1 \simeq 7 \pm 0.4$ eV, $\delta_1 \simeq 5 \pm 0.3$ and $P_2 \simeq (2 \pm 0.2) \times 10^{12}$ Pa, $T_2 \simeq 8 \pm 0.5$ eV, $\delta_2 \simeq 7 \pm 0.5$ are reached at $r = 3 \mu\text{m}$ prior to and immediately after the implosion, respectively.

Now let us analyze parameters of the SSW, which could explain the destruction of the central part of optical fiber, graphite rods, and Al wire. The length of the damaged part in the case of fiber ($r = 0.5$ mm) and Al wire ($r = 0.25$ mm) was $L \sim 1$ mm. In the case of graphite rods, it was difficult to estimate the length of the damaged part because the remaining part of the rod also was shattered into small pieces inside the shrink tube. The energy that is required for complete evaporation of the central part of the fiber and Al wire can be estimated as ~ 4.2 J and ~ 4.9 J, respectively. Let us consider the case of Al wire, which requires a larger energy deposited by the SSW that experience reflection from the wire surface. Using the results of simulations, which give $P \approx 2 \times 10^{10}$ Pa at $r = 0.25$ mm, one obtains a pressure at the Al surface of $P_{Al} = 4.2 \times 10^{10}$ Pa, $\delta = 2.1$ behind the SSW front, velocity of the water–Al wire boundary $U_{Al} \approx 2.2 \times 10^3$ m/s, and velocity of the SSW front in aluminum $D_{Al} \approx 8 \times 10^3$ m/s. The energy flux through the surface $S = 2\pi rL$ is $W = P_{Al} U_{Al} S$, and the duration of the energy transfer to the Al wire can be estimated as $T \approx r_{Al}/D_{Al}$. Thus, the energy which is transferred to the Al wire is $\Delta E \approx P_{Al} U_{Al} S T \approx 6.4$ J. Similar estimates showed that in the case of the fiber, the energy delivered by the SSW is also sufficient for its destruction. In the case of the 0.6 mm-diameter Cu wire, the energy delivered by the SSW (3.7 J) is not sufficient for its evaporation (13.8 J) because of the larger reflection coefficient of the SSW and density of the wire. Indeed, the 0.6 mm-diameter Cu wire was not destroyed in the experiment.

To conclude, the results of the sub-microsecond underwater electrical explosion of a spherical wire array produced by a generator with a stored energy ≤ 6 kJ showed that this approach can be used to generate an extreme state of water characterized by a pressure, temperature, and compression of the water in the vicinity of the origin of the implosion of $(2 \pm 0.2) \times 10^{12}$ Pa, 8 ± 0.5 eV, and 7 ± 0.5 , respectively.

This research was supported by the Israeli Science Foundation Grant No. 1044/08.

- ¹M. K. Matzen, M. A. Sweeney, R. G. Adams *et al.*, *Phys. Plasmas* **12**, 055503 (2005).
²N. Goldman, E. J. Reed, I.-F. W. Kuo, L. E. Fried, C. J. Mundy, and A. Curioni, *J. Chem. Phys.* **130**, 124517 (2009).
³V. E. Fortov and I. T. Iakubov, *The Physics of Non-Ideal Plasma* (World Scientific, Singapore, 2000).
⁴R. P. Drake, *Phys. Plasmas* **16**, 055501 (2009).
⁵R. Chau, A. C. Mitchel, R. W. Minich, and W. J. Nellis, *J. Chem. Phys.* **114**, 1361 (2001).
⁶P. M. Celliers, G. W. Collins, D. C. Hicks *et al.*, *Phys. Plasmas* **11**, L41 (2004).

- ⁷D. H. Dolan, M. D. Knudson, C. A. Hall, and C. Deeney, *Nat. Phys.* **3**, 339 (2007).
⁸V. E. Fortov, R. I. Ilkaev, V. A. Arinin *et al.*, *Phys. Rev. Lett.* **99**, 185001 (2007).
⁹S. Bouquet, C. Stehle, M. Koenig *et al.*, *Phys. Rev. Lett.* **92**, 225001 (2004).
¹⁰T. Pezeril, G. Saini, D. Veysset *et al.*, *Phys. Rev. Lett.* **106**, 214503 (2011).
¹¹A. F. Gefen, S. Efimov, L. Gilburd, G. Bazilitski, V. Tz. Gurovich, and Ya. E. Krasik, *Phys. Plasmas* **18**, 062701 (2011).
¹²A. Grinenko, V. Tz. Gurovich, and Ya. E. Krasik, *Phys. Plasmas* **14**, 012701 (2007).
¹³A. Grinenko, Ya. E. Krasik, S. Efimov, A. Fedotov, V. Tz. Gurovich, and V. I. Oreshkin, *Phys. Plasmas* **13**, 042701 (2006).
¹⁴S. Efimov, L. Gilburd, A. Fedotov-Gefen, V. Tz. Gurovich, J. Felsteiner, and Ya. E. Krasik, *Int. J. Shock Waves Detonat. Explos.* **22**, 207 (2012).
¹⁵V. I. Oreshkin, S. A. Chaikovsky, N. A. Ratakhin, A. Grinenko, and Ya. E. Krasik, *Phys. Plasmas* **14**, 102703 (2007).
¹⁶A. Fedotov, D. Sheftman, V. Tz. Gurovich, S. Efimov, G. Bazilitski, Ya. E. Krasik, and V. I. Oreshkin, *Phys. Plasmas* **15**, 082704 (2008).
¹⁷G. B. Whitham, *Linear and Nonlinear Waves* (John Wiley and Sons, New York, 1974).
¹⁸L. D. Landau and E. M. Lifshiz, *Fluid Mechanics* (Butterworth-Heinemann, Oxford, UK, 2005).
¹⁹I. V. Sokolov, *Sov. Phys. Usp.* **33**, 960 (1990).